JOURNAL OF OPTOELECTRONICS AND ADVANCED MATERIALS Vol. 9, No. 8, August 2007, p. 2321 - 2326

All-optical microwave photonic filters using a Hi-Bi chirped fiber Bragg grating

G. NING*, P. SHUM, S. ADITYA
Network Technology Research Centre, Nanyang Technological University, 50 Nanyang Drive, Research Techno Plaza, Singapore – 637553

We propose novel microwave photonic notch filter configurations using high-birefringence (Hi-Bi) chirped fiber Bragg grating (CFBG), together with their application in a 20 km single mode fiber (SMF) radio-over-fiber (RoF) link. Expressions are derived for 2-tap low-pass and bandpass filter transfer functions, including the effect of the fiber in the RoF link and the modulator chirp parameter. We demonstrate that the effect of chromatic dispersion due to the Hi-Bi CFBG can be either reduced or enhanced in a RoF link and that this effect can be used to improve the filter performance in a RoF link. Measured results are presented for both low pass and bandpass filter operations, including the effect of reduced or enhanced chromatic dispersion. A notch rejection greater than 30 dB and tuning of free spectral range (FSR) by tuning the Hi-Bi CFBG are demonstrated. The filter configurations are free from optically coherent interference and phase noise.

(Received December 7, 2006; accepted June 27, 2007)

Keywords: Microwave photonics, Radio-over-fiber, High-birefringence, Chirped fiber Bragg grating

1. Introduction

Microwave and millimeter-wave signals distributed over optical fibers are of great interest for many applications such as broad-band wireless access networks, wireless sensor networks, and satellite communication systems. There are many advantages of all-optical microwave filters. These include ability to directly process microwave and millimeter-wave signals in the optical domain [1]-[2], large time-bandwidth products, insensitivity to electromagnetic interference, low loss, and lightweight. A number of low pass microwave photonic filters have been reported in the literature [3]-[8]. They are required to achieve optically incoherent summing of two light beams. To overcome the optical coherence problem, either a laser array is used [3], or the coherence time of the light source is kept smaller than the minimum delay time of the filter [4]. Incoherent summing has also been achieved by using a Hi-Bi fiber [5]; however, such a filter cannot be tuned easily and needs a long segment of Hi-Bi fiber to achieve a small free spectral range (FSR) value. A step tuneable design with a tunable laser and uniform Hi-Bi gratings has been reported in [6]. A continuously tunable design, using a Hi-Bi CFBG in a double-pass connection, has been reported in [7]. The latter design suffers from a number of problems. First, it requires a polarization beam splitter with a low signal to noise ratio; second, some phase noise will be introduced by the crosstalk in the double-pass connection when the chirped grating is tuned; finally, the chromatic dispersion in the CFBG can result in carrier suppression effect [8]. Achieving a bandpass response in microwave photonic filters is more difficult than achieving a low-pass response. A bandpass filter has been reported in [9] by passing phase-modulated optical signal through a length of Hi-Bi fiber, followed by dispersive standard single mode fiber (SMF) to eliminate the baseband resonance. However, this configuration requires rather long length of Hi-Bi fiber to achieve small FSR values and it has poor tunability.

In this paper, we propose novel microwave photonic notch filters using a Hi-Bi CFBG. Both low pass and bandpass filter functions are demonstrated. The configuration, shown in Fig. 1 (a) and explained in detail in the next section, is free from the problem of optically coherent interference. Depending on the type of modulation, phase or intensity, one can achieve bandpass or low-pass filter response, respectively. The dispersion of the CFBG eliminates the low pass resonance for the case of phase modulation, enabling bandpass operation. Compared to [7], this configuration does not use a polarization beam splitter (PBS) or a double-pass connection; therefore the corresponding problems of signal to noise degradation and cross-talk, respectively, are avoided. Compared to [9], the Hi-Bi CFBG avoids the use of Hi-Bi fiber and offers easy tunabilty. Next, using the configuration shown in Fig. 1(b), incorporating a 20 km long SMF, we demonstrate that the chromatic dispersion due to the Hi-Bi CFBG can either be reduced or enhanced in an RoF link and that this effect can be used to improve the filter performance in an RoF link. This observation is significant since microwave photonic filters are strongly proposed for applications in RoF links. For both configurations (Figs. 1 a and b) expressions are derived here for low-pass and bandpass filter transfer functions, including the effect of the modulator chirp parameter for the case of intensity modulation. Measured results are presented for both low pass and bandpass filter operations, including the effect of reduced or enhanced chromatic dispersion for the case when the SMF is included. Measured results show a notch rejection greater than 30 dB and an easily tunable free spectral range (FSR) by tuning the Hi-Bi CFBG. In most cases, measured results compare very well with the calculated results.

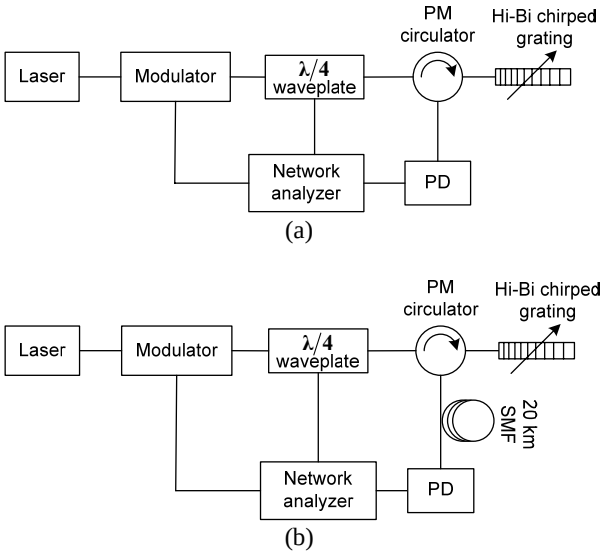

Fig. 1. Experimental setup; (a) low pass and bandpass notch filters using a Hi - Bi CFBG; (b) filters incorporating a 20 km SMF.

2. Experimental setup and principle of operation

The experimental set-up for the filters is shown in Fig. 1 (a). An RF signal drives a modulator which has Hi-Bi pigtails, modulating the output of a laser (ANDO AQ8201-13A). The output of the modulator is launched into a $\lambda/4$ waveplate which changes the input linear state of polarization (SOP) into a circular one. The output signal from the $\lambda/4$ waveplate is connected to a Hi-Bi CFBG through a polarization maintaining (PM) circulator. The final output of the PM circulator is fed to a photodetector (PD), which is followed by a network analyzer. If the modulator is used as an intensity modulator, the filter function achieved is low pass. If the modulator is used as a phase modulator, the filter function achieved is bandpass. The experimental setup shown in Fig. 1 (b) includes a 20 km SMF representing a RoF link; here, the final output signal from the PM circulator is first fed to a 20 km SMF and then connected to the PD.

The differential group delay (DGD) between the two orthogonal SOPs at the output of the PM circulator consists of two parts: one ($\Delta\tau_0$) is caused by the birefringence of the pigtails of the PM circulator and the Hi-Bi CFBG, and the other ($\Delta\tau_d$) is caused by the Hi-Bi CFBG. A Hi-Bi CFBG behaves as two virtual CFBGs corresponding to the two orthogonal polarization axes: fast and slow. The wavelength and group delay difference between the spectra of the two gratings is determined by the Hi-Bi fiber's effective refractive index difference between the fast and slow axes. For a given signal wavelength which lies within the common bandwidth of the two gratings, after the signal is reflected by the Hi-Bi chirped grating, DGD occurs between the two parts of the signal travelling along the fast and slow axes due to the group delay difference between the two chirped FBGs corresponding to the two polarization axes.

3. Principle of operation

(i) Phase modulation

A sinusoidal phase modulation of the optical electric field can be expressed as:

$$f(t) = \sqrt{P}_i \exp j\left(\omega_0 t + A\sin\omega_m t\right) \qquad (1)$$

where P_i is the output optical power from the laser, ω_0 is the angular frequency of the optical carrier, A is the modulation factor, and ω_m is the modulating angular frequency. In our system, the modulation frequency lies between 0.04 – 10 GHz. It is assumed that the modulator has a Hi-Bi pigtail and the SOP of the output light from the laser is optimally aligned to that of the modulator.

Eq. (1) can be expanded into a series of Bessel functions [10]:

$$f(t) = \sqrt{P_i}\sum_{i=-\infty}^{\infty}(j)^i J_i(A)\exp j\left(\omega_0 t + i\omega_m t\right) \qquad (2)$$

where J_i are Bessel functions of the first kind. In general, the signal consists of a series of sidebands with Bessel function amplitude coefficients. However, assuming that the modulation factor is small, the higher-order sidebands can be neglected; only the first-order upper and lower sidebands are retained in the following discussion. It is also assumed that the signal is excited equally in the two orthogonal polarizations, $\boldsymbol{\Omega}_+$ and $\boldsymbol{\Omega}_-$, corresponding to the fast and slow axis in the Hi-Bi CFBG. Then, the signal after propagation can be decomposed into two components: $f_{\Omega+}(t)$ and $f_{\Omega-}(t)$, corresponding to the two orthogonal polarizations. In the case when the short wavelength port of the Hi-Bi CFBG is connected to the circulator, the two components $f_{\Omega+}(t)$ and $f_{\Omega-}(t)$ can be written as:

$$f_{\Omega+}(t) = M\frac{\sqrt{P_i/2}}{\sqrt{2\pi}}\int_{-\infty}^{\infty} F(\omega-\omega_0)\exp\left[\left(j\Delta\tau_0\Delta\omega/2\right)+\left(j\Delta\tau_d\Delta\omega/2\right)-\left(jd_\rho\Delta\lambda\Delta\omega/2\right)\right]d\omega \qquad (3)$$

$$f_{\Omega-}(t) = M\frac{\sqrt{P_i/2}}{\sqrt{2\pi}}\int_{-\infty}^{\infty} F(\omega-\omega_0)\exp\left[-\left(j\Delta\tau_0\Delta\omega/2\right)-\left(j\Delta\tau_d\Delta\omega/2\right)-\left(jd_\rho\Delta\lambda\Delta\omega/2\right)\right]d\omega \qquad (4)$$

In Eqs. (3) and (4), $F(\omega-\omega_0)=\int_{-\infty}^{\infty} f(t)\exp\left[-j(\omega-\omega_0)t\right]dt$, M is a magnitude factor, $d_\rho = \left(2n_{eff}/c\right)\left(d\lambda_B/dz\right)^{-1}$ is the grating dispersion (ps/nm) [11], $\Delta\lambda$ is the chirped wavelength dependent on the modulation frequency ω_m

and is defined as $\Delta\lambda = 2\pi c\omega_m / \omega_0^2$, $\Delta\tau_0$ is the differential group delay (DGD) induced by the pigtails of the PM circulator and Hi-Bi chirped grating, and $\Delta\tau_d$ is the DGD induced by the Hi-Bi CFBG. By assuming the responsivity of the photodiode to be R, the RF output current, corresponding to the two orthogonal components, is given as:

$$I(t) = \frac{1}{4} RP_i M^2 \begin{Bmatrix} 4\left[J_0(A)\right]^2 + 4J_0(A)J_1(A)\sin\left(d_\rho \omega_m^2 \lambda^2 / 4\pi c\right)\cos\left[\omega_m\left(t + \Delta\tau_d/2 + \Delta\tau_0/2\right)\right] \\ +4J_0(A)J_1(A)\sin\left(d_\rho \omega_m^2 \lambda^2 / 4\pi c\right)\cos\left[\omega_m\left(t - \Delta\tau_d/2 - \Delta\tau_0/2\right)\right] \end{Bmatrix} \quad (5)$$

In (5), λ is the operating wavelength of the laser source and c is the speed of light in fiber (2×10^8 m/s). Comparing Eq. (5) with the RF input voltage in Eq. (1), the transfer function for the microwave filter can be written as:

$$\left|H(\omega_m)\right| = RM^2 \sin\left(d_\rho \omega_m^2 \lambda^2 / 4\pi c\right)\left|\cos\left[\omega_m\left(\Delta\tau_0 + \Delta\tau_d\right)/2\right]\right| \quad (6)$$

In Eq. (6), the magnitude of the filter response function consists of a product of two parts: $\sin\left(d_\rho \Delta\lambda \omega_m\right)$ and $\left|\cos\left[\omega_m\left(\Delta\tau_0 + \Delta\tau_d\right)/2\right]\right|$. The former part corresponds to a bandpass response. As explained in the previous discussion, the time difference between the two components $f_{\Omega+}(t)$ and $f_{\Omega-}(t)$ is

$$\Delta\tau = \Delta\tau_0 + \Delta\tau_d \quad (7)$$

where $\Delta\tau_0$ is the fixed time delay due to the Hi-Bi pigtails of the circulator and Hi-Bi CFBG. $\Delta\tau_0$ is as small as about 4 ps and can be neglected compared with the DGD induced by the Hi-Bi CFBG.

When the long wavelength port of the Hi-Bi CFBG is connected to the circulator, the transfer function is very similar to that in Eq.(6), and can be expressed as

$$\left|H(\omega_m)\right| = RM^2 \sin\left(d_\rho \omega_m^2 \lambda^2 / 4\pi c\right)\left|\cos\left[\omega_m\left(\Delta\tau_0 - \Delta\tau_d\right)/2\right]\right| \quad (8)$$

In this case, the time difference between the two components $f_{\Omega+}(t)$ and $f_{\Omega-}(t)$ is $\Delta\tau = \Delta\tau_0 - \Delta\tau_d$.

Similarly, for the configuration of Fig. 1 (b), when a length l of SMF is included in the design, for the case when the short wavelength port of the Hi-Bi CFBG is connected to the circulator, the filter transfer function can be obtained as:

$$\left|H(\omega_m)\right| \propto \sin\left[-\left(d_\rho \omega_m^2 \lambda^2 / 4\pi c\right) + \left(\omega_m^2 \lambda^2 Dl / 4\pi c\right)\right]\left|\cos\left[\omega_m\left(\Delta\tau_d + \Delta\tau_0\right)/2\right]\right| \quad (9)$$

In (9), D is the dispersion parameter of the single mode fiber (SMF). However, when the long wavelength port of the Hi-Bi CFBG is connected to the circulator, the filter transfer function is given by

$$\left|H(\omega_m)\right| \propto \sin\left[\left(d_\rho \omega_m^2 \lambda^2 / 4\pi c\right) + \left(\omega_m^2 \lambda^2 Dl / 4\pi c\right)\right]\left|\cos\left[\omega_m\left(\Delta\tau_d - \Delta\tau_0\right)/2\right]\right| \quad (10)$$

Eqs. (9) and (10) show that the fiber dispersion may either reduce or enhance the effect of the grating dispersion.

(ii) Intensity modulation

For the case of intensity modulation, experiment setup is the same as that in Fig.1 (a), except that the intensity modulation replaces the phase modulation. A sinusoidal intensity modulation of the optical electric field can be expressed as:

$$f(t) = \sqrt{P_i}\sqrt{1 + m\cos\left(\omega_m t\right)}\cos\left(\omega_0 t\right) \quad (11)$$

where m is the phase modulation index, P_i is the output optical power from the laser, ω_0 is the angular frequency of the optical carrier, A is the modulation factor, and ω_m is the modulating angular frequency. Under small signal condition (m<<1), Eq. (11) can be approximated as:

$$f(t) = \sqrt{P_i}\left(1 + \frac{1}{2} m\cos\omega_m t\right)\cos\omega_0 t = \sqrt{P_i}\begin{bmatrix} \cos\omega_0 t + \frac{m(1+ja)}{4}\cos\left(\omega_0 + \omega_m\right)t \\ + \frac{m(1+ja)}{4}\cos\left(\omega_0 - \omega_m\right)t \end{bmatrix} \quad (12)$$

Here α is a parameter that relates the instantaneous intensity induced phase variation of the modulated light; α is also known as chirp parameter [12][13]. It is first assumed that the short wavelength port of the Hi-Bi CFBG is connected to the circulator. Then, similar to the case of phase modulation, the two orthogonally polarized components $f_{\Omega+}(t)$ and $f_{\Omega-}(t)$ are written as:

$$f_{\Omega+}(t) = M\frac{\sqrt{P_i}}{\sqrt{2}}\begin{Bmatrix} \cos\left(\omega_0 t\right) + \frac{m\sqrt{1+\alpha^2}}{4}\cos\left\{\omega_0 t + \omega_m\left[t + \left(\Delta\tau_0 + \Delta\tau_d\right)/2 - d_\rho \Delta\lambda/2 - \arctan(\alpha)\right]\right\} \\ + \frac{m\sqrt{1+\alpha^2}}{4}\cos\left\{\omega_0 t - \omega_m\left[\left(t + \left(\Delta\tau_0 + \Delta\tau_d\right)/2 + d_\rho \Delta\lambda/2 + \arctan(\alpha)\right)\right]\right\} \end{Bmatrix} \quad (13)$$

$$f_{\Omega-}(t) = M\frac{\sqrt{P_i}}{\sqrt{2}}\begin{Bmatrix} \cos\left(\omega_0 t\right) + \frac{m\sqrt{1+\alpha^2}}{4}\cos\left\{\omega_0 t + \omega_m\left[t - \left(\Delta\tau_0 + \Delta\tau_d\right)/2 - d_\rho \Delta\lambda/2 - \arctan(\alpha)\right]\right\} \\ + \frac{m\sqrt{1+\alpha^2}}{4}\cos\left\{\omega_0 t - \omega_m\left[t - \left(\Delta\tau_0 + \Delta\tau_d\right)/2 + d_\rho \Delta\lambda/2 + \arctan(\alpha)\right]\right\} \end{Bmatrix} \quad (14)$$

Assuming the responsivity of the photodiode to be R, we can express the RF output current as:

$$I(t) = \frac{1}{2} RP_i M^2 \cdot \begin{bmatrix} 1 + m\sqrt{1+\alpha^2}\cos\left[\left(d_\rho \omega_m^2 \lambda^2 / 4\pi c\right) + \arctan(\alpha)\right]\cos\left[\omega_m t + \left(\omega_m \Delta\tau_0/2\right) + \left(\omega_m \Delta\tau_d/2\right)\right] \\ m\sqrt{1+\alpha^2}\cos\left[\left(d_\rho \omega_m^2 \lambda^2 / 4\pi c\right) + \arctan(\alpha)\right]\cos\left[\omega_m t - \left(\omega_m \Delta\tau_0/2\right) - \left(\omega_m \Delta\tau_d/2\right)\right] \end{bmatrix} \quad (15)$$

Comparing the RF output current in Eq. (15) with the RF input voltage in Eq. (11), the transfer function for the microwave filter can be obtained as:

$$\left|H(\omega_m)\right| = \frac{RM^2}{2}\sqrt{1+\alpha^2}\left|\cos\left[\left(d_\rho\omega_m^2\lambda^2/4\pi c\right)+\arctan(\alpha)\right]\right|\left|\cos\left[\omega_m\left(\Delta\tau_0+\Delta\tau_d\right)/2\right]\right| \quad (16)$$

In Eq. (16), the magnitude of the filter response function consists of a product of $\left|\cos\left[\left(d_\rho\omega_m^2\lambda^2/4\pi c\right)+\arctan(\alpha)\right]\right|$ and $\left|\cos\left[\omega_m\left(\Delta\tau_0+\Delta\tau_d\right)/2\right]\right|$. Both parts correspond to a low pass response. Eq. (16) also shows that it is possible to compensate the effect of chromatic dispersion on the performance of the filter by using an optical modulator with adjustable chirp [14]. Next, when the long wavelength port of the Hi-Bi CFBG is connected to the circulator, the second part of the filter transfer function changes to $\left|\cos\left[\omega_m\left(\Delta\tau_0-\Delta\tau_d\right)/2\right]\right|$.

Next, one incorporates the effect of a length l of the SMF on the filter performance. For the case when the short wavelength port of the Hi-Bi CFBG is connected to the circulator, the filter transfer function can be obtained as

$$\left|H(\omega_m)\right| \propto \left|\cos\left[-\left(d_\rho\omega_m^2\lambda^2/4\pi c\right)+\left(\omega_m^2\lambda^2 Dl/4\pi c\right)+\arctan(\alpha)\right]\right|\left|\cos\left[\omega_m\left(\Delta\tau_d+\Delta\tau_0\right)/2\right]\right| \quad (17)$$

However, when the long wavelength port of the Hi-Bi CFBG is connected to the circulator, the filter transfer function is

$$\left|H(\omega_m)\right| \propto \left|\cos\left[\left(d_\rho\omega_m^2\lambda^2/4\pi c\right)+\left(\omega_m^2\lambda^2 Dl/4\pi c\right)+\arctan(\alpha)\right]\right|\left|\cos\left[\omega_m\left(\Delta\tau_d-\Delta\tau_0\right)/2\right]\right| \quad (18)$$

Eqs. (17) and (18) again show that the fiber dispersion may either reduce or enhance the effect of the grating dispersion.

4. Measured results and discussion

The Hi-Bi CFBG is written by exposing a hydrogen-loaded high-birefringence fibre to a 244 nm laser beam through a chirped phase mask. The length of the grating is about 7.7 cm. The reflectivity for fast and slow axis of the grating is shown in Fig. 2 (a). The 3-dB bandwidth for each axis is 1.53 nm, and the centre wavelengths are 1554.625 nm and 1555.02 nm for the fast and the slow axis, respectively. The reflectivity of the original grating is about 99.9% within the effective bandwidth. Fig. 2 (b) depicts the group delay for the slow and fast axis as well as the DGD in the common bandwidth (from 1554.25 nm to 1555.39 nm). It is clear that there are ripples in DGD value; the ripples are caused by the fact that the grating is fabricated without apodization. When the Hi-Bi CFBG is linearly stretched using a beam [15], the DGD will change as shown in Fig. 2 (b). The FSR of the filters can be tuned in this manner.

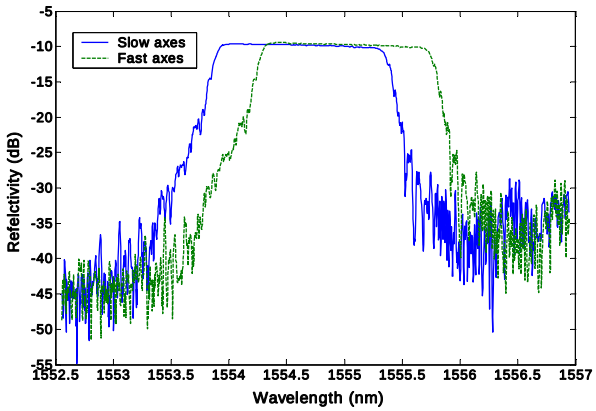

Fig. 2. (a) Measured reflectivity of the Hi-Bi chirped FBG.

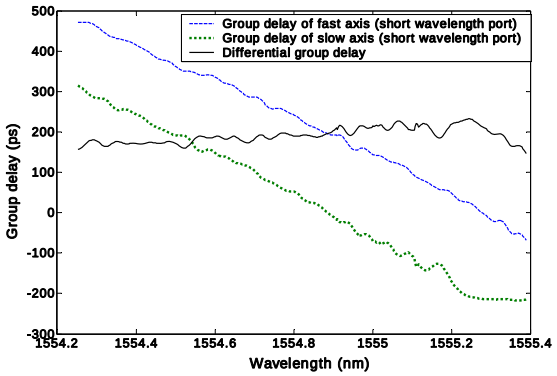

Fig. 2. (b) Measured group delay and differential group delay (DGD) for the Hi-Bi chirped FBG.

Results for the configuration shown in Fig. 1 (a), where a fiber length is not included in the set-up, are presented first. The operating wavelength of the laser is 1555.01 nm and the short wavelength port of the Hi-Bi CFBG is connected to the circulator. The measured low pass filter response is shown in Fig. 3 (a), with no tuning of the Hi-Bi chirped FBG. The measured DGD at this wavelength for the Hi-Bi chirped FBG is 211 ps and $\Delta\tau_0$ is about 3 ps, so the total DGD is about 214 ps. Using this value of total time delay, $\alpha = 0$, and $d_\rho = 400\ ps/nm$, the calculated results using Eq.(16) are also included in Fig. 3 (a). There is good agreement between the measured and calculated results. Since if the modulator is used as an intensity modulator, the filter function achieved is low pass, and if the modulator is used as a phase modulator, the filter function achieved is bandpass, we can show the comparison between bandpass filter and low pass filter response. Fig. 3 (b) shows the measured bandpass filter response obtained using phase

modulation. The calculated results using Eq. (6) with $\Delta\tau = 214$ ps again match well with the measured results.

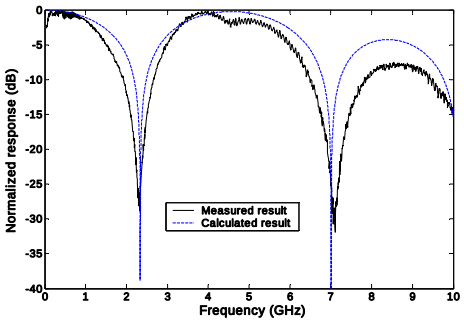

Fig. 3. (a). Measured and calculated low pass filter response without tuning the Hi-Bi chirped FBG (short wavelength port).

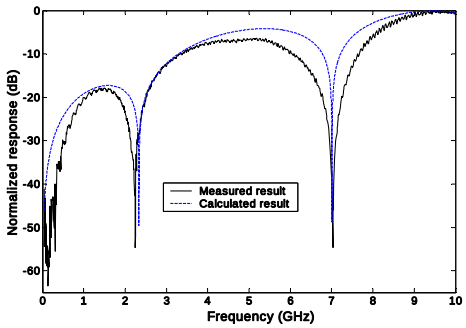

Fig. 3. (b). Measured and calculated bandpass filter response without tuning the Hi-Bi chirped FBG (short wavelength port).

Next, the Hi-Bi CFBG is tuned linearly to a longer wavelength of 1555.11 nm by using a beam [15]. The measured DGD at this wavelength is about 215 ps; together with $\Delta\tau_0 = 3$ ps, the total DGD is about 218 ps. This value is used for calculated results for low pass and bandpass filter responses presented in Fig. 4 (a) and 4 (b), respectively. Fig. 4 shows that the calculated results agree reasonably well with the measured results for both low pass and bandpass filters.

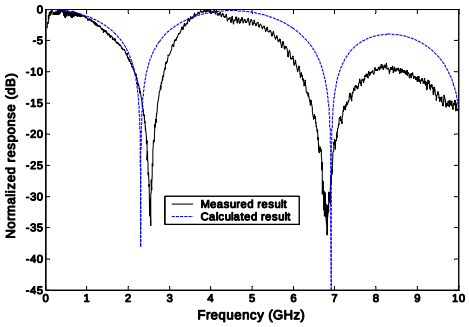

Fig. 4. (a). Measured and calculated low pass filter response when the grating is tuned to a longer wavelength of 1555.11 nm (short wavelength port).

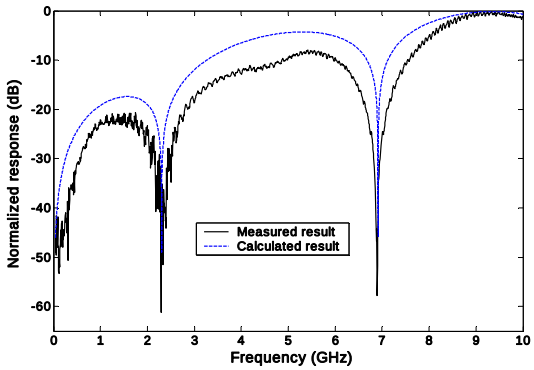

Fig. 4. (b). Measured and calculated bandpass filter response when the grating is tuned to a longer wavelength of 1555.11.

Presented next are results for the configuration shown in Fig. 1 (b), where a 20 km fiber length is included in the set-up. Fig. 5 (a) shows the low pass filter response when the short wavelength port of the Hi-Bi CFBG is connected to the circulator. It is seen that the magnitude response of the filter is enhanced compared with that in Fig. 3 (a). This is seen clearly around 9 GHz. This improvement is because of the reduction in the effect of dispersion of the grating due to the dispersion of the fiber (see Eq. (17)). However, there is more phase noise present due to the 20 km SMF link. The value of total DGD used in Eq. (17) for calculated results in Fig. 5 (a) is 214 ps ($\Delta\tau_d + \Delta\tau_0$); the value of dispersion parameter D is 17 ps/nm.km. On the other hand, when the long wavelength port of the Hi-Bi CFBG is connected to the circulator, as shown in Fig. 5 (b), the magnitude response is much worse compared to that in Fig.3 (a), since in this case the dispersion of the grating and the fiber add to each other (see Eq. (18)). The value of total DGD used in Eq. (18) for calculated results in Fig. 5 (b) is 208 ps ($\Delta\tau_d - \Delta\tau_0$). Accordingly, the FSR value seen in Fig. 5 (b) is slightly larger than that in Fig. 5 (a). Moreover, although, the 20 km SMF induces phase noise which affects carrier suppression effect due to the chromatic dispersion, the measured FSR agrees with the calculated FSR, as shown in Fig. 5 (b).

nm (short wavelength port).

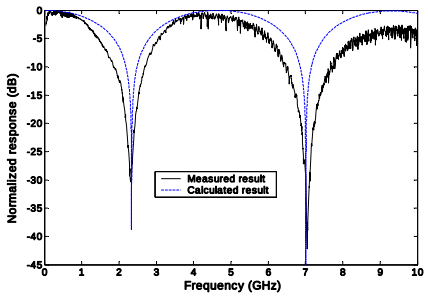

Fig. 5. (a). Measured and calculated low pass filter response including a 20 km SMF; short wavelength port (no tuning of FBG).

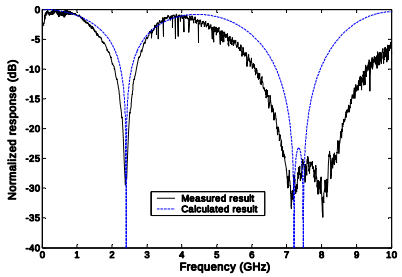

Fig. 5. (b). Measured and calculated low pass filter response including a 20 km SMF; long wavelength port (no tuning of FBG).

Fig. 6 shows the bandpass filter response including the effect of 20 km SMF. When the short wavelength port of the Hi-Bi CFBG is connected to the circulator, Fig. 6 (a) shows that the magnitude response of the filter degrades a bit compared with that in Fig.3 (b); this is clear around 1-2 GHz frequency range. This is because of the phase modulation coupled with CD compensation, as indicated in Eq. (9). Fig. 6 (b) shows that when the long wavelength port of the Hi-Bi CFBG is connected to the circulator, the magnitude response around 1-2 GHz improves compared to that in Fig.3 (b), since, as indicated in Eq. (10), the CD is enhanced in this case.

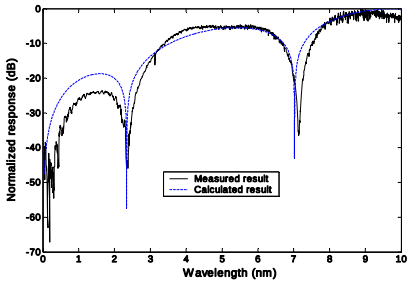

Fig. 6. (a). Measured and calculated bandpass filter response including a 20 km SMF; short wavelength port (no tuning of FBG).

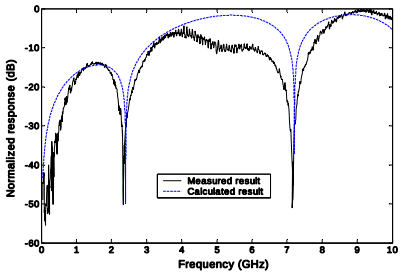

Fig. 6. (b). Measured and calculated bandpass filter response including a 20 km SMF; long wavelength port (no tuning of FBG).

It should be pointed out that if the Hi-Bi linearly chirped FBG is tuned nonlinearly [16] or one uses a Hi-Bi nonlinearly chirped FBG [17] with linear tuning, both the CD and the DGD values can be tuned over a longer range.

5. Conclusion

All-optical low pass and bandpass microwave filter configurations, together with their application in a 20 km single mode fiber (SMF) RoF link have been demonstrated. The baseband resonance is eliminated by the use of phase modulation combined with the dispersion of the Hi-Bi chirped FBG and the fiber. For both types of filters, it is demonstrated that the dispersion of the grating may be reduced or enhanced by the presence of fiber. This modification of dispersion effect can be used to improve the filter performance in a RoF link. In general, there is reasonably good agreement between the measured results and the calculated results based on the expressions developed here.

References

[1] J. Capmany, B. Ortega, D. Pastor, S. Sales, J. Lightwave Technol. **23**, 702-723 (2005).
[2] R. A. Minasian, Trans. Microw. Theory Technol. **54**, 832-846 (2006).
[3] D. Pastor, J. Capmany, Electron. Lett. **34**, 1684-1685 (1998).
[4] E. H. W. Chan, K. E. Alameh, J. A. R. Minasian, J. Lightwave Technol. **20**, 1962-1967 (2002).
[5] W. Zhang, J. A. R. Williams,I. Bennion, Electron. Lett. **35**, 2133-2134 (1999).
[6] W. Zhang, J. A. R. Williams, I. Bennion, Photon. Technol. Lett. **13**, 523-525 (2001).
[7] Xiaoke Yi, Chao Lu, et al., Photon. Technol. Lett. **15**, 754-756 (2003).
[8] J. Capmany, D. Pastor, B. Ortega, Trans. Microw. Theory Technol. **47**, 1321-1326 (1999).
[9] J. Wang, J. P. Yao, Photon. Technol. Lett. **17**, 1737-1739 (2005).
[10] A. R. Chraplyvy, R. W. Tkach, L. L. Buhl, R. C. Alferness Electron. Lett. **22**, 409-410 (1986).
[11] Erdogan, Turan, J. Lightwave Technol. **15**, 1277-1294 (1997).
[12] F. Koyame, K. Iga, J. Lightwave Technol. **6**, 87-93 (1988).
[13] F. Devaux, Y. Sorel, J. F. Kerdiles, J. Lightwave Technol.**11**, 1937-1940 (1993).
[14] P. Jiang, A. C. Donnell, Photon Technol Lett. **8**, 1319-1321 (1996).
[15] Zixiang. Qin, Q. Zeng, X. Yang, D. Feng, L. Ding, G. Kai, Z. Liu, S. Yuan, X. Dong, N. Liu, Photon. Technol. Lett. **13**, 326-328 (2001).
[16] X. Y. Dong, N. Q. Ngo, P. Shum, J. H. Ng, X. Yang, G. Ning, C. Lu, Photon. Tech. Lett. **16**, 846-848 (2004).
[17] S. Lee, R. Khosravani, at el., "Adjustable compensator of polarization mode dispersion using a high birefringence nonlinearly chirped fiber Bragg grating," Photon. Technol. Lett. **11**, 1277-1279 (1999).

*Corresponding author: ngxstone@pmail.ntu.edu.sg